Neoplasia • Vol. 4, No. 3, 2002, pp. 204–217

www.nature.com/neo



# Insulin-Like Growth Factor-1 Inscribes a Gene Expression Profile for Angiogenic Factors and Cancer Progression in Breast Epithelial Cells[1]

*J.S. Oh*, J.E. Kucab[†,‡], P.R. Bushel[§], K. Martin[§], L. Bennett[§], J. Collins[§], R.P. DiAugustine*, J.C. Barrett[¶], C.A. Afshari[§] and S.E. Dunn[†,‡]*

*Laboratory of Molecular Carcinogenesis, Hormones and Cancer Group, National Institute of Environmental Health Sciences (NIEHS), Research Triangle Park, NC, USA; [†]Functional Genomics Program, North Carolina State University, Raleigh, NC, USA; [‡]British Columbia Research Institute for Children's and Women's Health, Vancouver, BC, Canada; [§]Laboratory of Molecular Carcinogenesis, Microarray Group, NIEHS, Bethesda, MD, USA; [¶]Laboratory of Biosystems and Cancer, National Cancer Institute, Bethesda, MD, USA

## Abstract

**Activation of the insulin-like growth factor-1 receptor (IGF-1R) by IGF-1 is associated with the risk and progression of many types of cancer, although despite this it remains unclear how activated IGF-1R contributes to cancer progression. In this study, gene expression changes elicited by IGF-1 were profiled in breast epithelial cells. We noted that many genes are functionally linked to cancer progression and angiogenesis. To validate some of the changes observed, the RNA and/or protein was confirmed for c-*fos*, cytochrome P450 1A1, cytochrome P450 1B1, interleukin-1 beta, fas ligand, vascular endothelial growth factor, and urokinase plasminogen activator. Nuclear proteins were also temporally monitored to address how gene expression changes were regulated. We found that IGF-1 stimulated the nuclear translocation of phosphorylated AKT, hypoxic-inducible factor-1 alpha, and phosphorylated cAMP-responsive element-binding protein, which correlated with temporal changes in gene expression. Next, the promoter regions of IGF-1–regulated genes were searched *in silico*. The promoters of genes that clustered together had similar regulatory regions. In summary, IGF-1 inscribes a gene expression profile relevant to cancer progression, and this study provides insight into the mechanism(s) whereby some of these changes occur.**

*Neoplasia* (2002) **4,** 204–217 DOI: 10.1038/sj/neo/7900229

**Keywords:** microarray, insulin-like growth factor-1 receptor, AKT, transcription factors, breast cancer.

## Introduction

The insulin-like growth factor-1 (IGF-1) and its receptor (IGF-1R) are associated with many types of human cancers, including those derived from lung, breast, and prostate. Based upon several epidemiological studies, elevated levels of serum IGF-1 are linked to an increased risk of developing ductal carcinoma *in situ* (DCIS) [1], as well as invasive breast [2], colon [3], lung [4], and prostate cancers [5]. These data suggest that IGF-1/IGF-1R is potentially a useful molecular target for cancer intervention. In support of this idea, there are several reports demonstrating that the disruption of serum IGF-1 slows tumorigenesis. For example, mice with reduced serum IGF-1 have slower-growing tumors compared with wild-type mice [6]. We also showed that attenuation of IGF-1 suppresses the progression of bladder cancer in mice [7]. The importance of activated IGF-1R in cancer progression is further underscored by its role in cellular transformation [8] and maintenance of the malignant phenotype. To illustrate this point, the malignant phenotype is disrupted by antisense expression plasmids [9], antisense oligodeoxynucleotides [10], a neutralizing antibody [11], and dominant negative mutants to the IGF-1R [12]. Our laboratory also demonstrated that inhibition of IGF-1R with a dominant negative mutant suppresses invasion and metastases of breast cancer in nude mice [13]. More recently, it was reported that antisense oligodeoxynucleotides to IGF-1R caused regression of astrocytomas in humans [14]. These studies collectively point toward IGF-1/IGF-1R as being important for the development and progression of a number of types of cancer. Thus, disrupting IGF-1R or one of its critical signal transduction pathways could have applications for cancer intervention.

IGF-1 binds to IGF-1R and triggers a cascade of signal transduction events, including activation of the phosphatidyl

Abbreviations: AP-1, activating protein-1; BPAG, bullous pemphigoid antigen; P-CREB, cAMP-responsive element-binding protein; DCIS, ductal carcinoma *in situ*; FKHR, forkhead transcription factor; htert, human telomerase reverse transcriptase; HIF-1$\alpha$, hypoxic-inducible factor-1 alpha; IGF-1R, insulin-like growth factor-1 receptor; MMP, matrix metalloproteinase; PI3K, phosphatidyl inositol-3 kinase; PDAR, predeveloped assay reagent; uPA, urokinase plasminogen activator; VEGF, vascular endothelial growth factor

Address all correspondence to: Dr. Sandra E. Dunn, Department of Pediatrics, British Columbia Institute for Children's and Women's Health, 950 West 28th Avenue, Vancouver, BC, Canada V5Z 4H4. E-mail: sedunn@interchange.ubc.ca

[1]This work was sponsored, in part, by the National Institute of Health, National Institute of Environmental Health Sciences, K22 award to S.E.D. (5K22ES00337-02) and a National Cancer Institute, Breast Cancer Think Tank grant awarded to S.E.D., C.A.A., R.P.D., and J.C.B.

Received 27 July 2001; Accepted 15 October 2001.

inositol-3 kinase (PI3K) pathway that leads to phosphorylation of AKT (P-AKT), rendering it in an active conformation. PI3K stimulates the P-AKT through either the integrin-linked kinase [15] or phosphoinositide-dependent kinase [16]. Upon activation, P-AKT rapidly responds to the IGF-1 signal by initially associating with the plasma membrane where it binds to phosphatidylinositol 3,4,5-Tris phosphate or phosphatidylinositol 3,4 bisphosphate [17]. Thereafter, P-AKT leaves the plasma membrane and quickly translocates into the nucleus [18]. Inhibition of PI3K signaling with LY294002 inhibits the nuclear translocation of P-AKT and correlates with a suppression of cell proliferation [19]. AKT is also widely recognized for the ability to inhibit apoptosis as a cellular response to insulin [20]. Furthermore, we previously reported that IGF-1/AKT signaling facilitates cancer invasion [21] while several other laboratories find that AKT is important for the regulation of angiogenesis (reviewed in Ref. [22]). AKT regulates angiogenesis in part by stimulating the hypoxic-inducible factor-1 alpha (HIF-1$\alpha$) and the subsequent production of the vascular endothelial growth factor (VEGF) [23]. It is noteworthy that both hypoxia and IGF-1 induce the nuclear accumulation of HIF-1$\alpha$ [24]. Hence, AKT is becoming a common intermediate in the regulation of angiogenesis by controlling transcription factors such as HIF-1$\alpha$.

AKT is a serine/threonine kinase with the propensity to regulate cellular processes by phosphorylating transcription factors, thereby serving as a nuclear messenger for controlling IGF-1–induced gene expression (Figure 1). P-AKT binds and phosphorylates transcription factors such as cAMP-responsive element binding (CREB), FKHRL1, AFX, and NFkB. There is also evidence that activation of AKT signaling by insulin stimulates activating protein-1 (AP-1) transactivation by inhibiting glycogen synthase kinase-3 [25]. In the case of CREB, AKT binds this transcription factor, resulting in phosphorylation of serine 133 [26]. The phosphorylation of CREB is sufficient for its association with the coactivators CREB-binding protein (CBP)/p300 and for transactivation of CRE-responsive genes such as c-*fos* [27]. CREB becomes phosphorylated by a variety of cellular stimuli, including hypoxia [28] and IGF-1 [29]. The phosphorylation of CREB by hypoxia depends upon AKT [30]. Hence, activation of HIF-1$\alpha$, CREB, and AP-1 by AKT positively regulates gene expression. Alternatively, AKT negatively regulates gene expression in some cases by phosphorylating the forkhead transcription factors FKHR, FKHRL1, and AFX. AKT negatively regulates the mRNA expression of fas ligand and the insulin-binding protein-1 by phosphorylating FKHRL1 [31] and AFX [32], respectively. The phosphorylation of FKHRL1 and AFX results in transport of these transcription factors out of the nuclear compartment, and the suppression of genes that positively regulate apoptosis. Thus, AKT is emerging as an important molecule for mediating nuclear transcription factors and the regulation of gene expression by stimuli such as IGF-1.

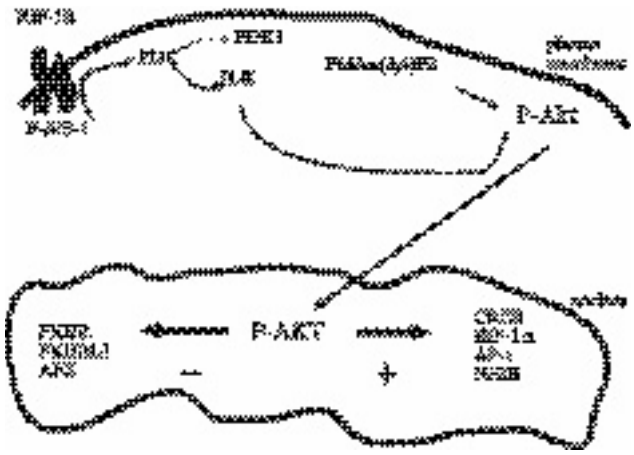


**Figure 1.** *A schematic representation of IGF-1 signal transduction leading from the IGF-1R receptor to the eventual regulation of gene expression by P-AKT. The activation of AKT by phosphorylation by phosphatidyl inositide-dependent kinase (PDK) or integrin-linked kinase (ILK) results in localization to the plasma membrane followed by trafficking into the nucleus. P-AKT modifies the transcription activation of nuclear proteins by phosphorylating them at serine and threonine residues. As a result of AKT phosphorylation, transcription factors such as CREB, HIF-1α, AP-1, and NFαB are activated; therefore, binding of these transcription factors induces gene expression. Alternatively, the forkhead transcription factors (FKHR, FHKRL1, and AFX) are phosphorylated by AKT at serine and threonine residues, although in this case transactivation is inhibited because the modified proteins are expelled from the nucleus.*

A question that remains unanswered is how the IGF-1/IGF-1R facilitates cancer progression because carcinogenesis is a complex process that involves the stimulation of cell growth signals, suppression of apoptosis, and the acquisition of a malignant phenotype. With the advent of microarrays and bioinformatics, we are poised to begin to decipher such a complex biological problem. In this study, we made temporal comparisons using the immortalized breast epithelial cell 184htert and analyzed changes in gene expression by microarray. We selected the 184htert cell line because it loosely represents a preneoplastic stage of breast cancer. Profiling a cell line such as the 184htert has a recognizable distinction to other microarray reports where normal and cancer cell lines were compared [33]. Given the clinical, basic, and epidemiological support for IGF-1/IGF-1R in breast cancer, we recognized a need for defining the influence of IGF-1 at an early stage with the hope of finding avenues for intervention. Therefore, the model provided an opportunity for studying the effect of IGF-1 on early stage of breast cancer progression. The activation of oncogenes, loss of tumor suppressor genes, and genomic instability associated with breast cancer cell lines may confound our ability to measure the effect of IGF-1 on the regulation of gene expression. In this study, we found that IGF-1 induces several genes involved in cancer progression particularly those related to angiogenesis. Furthermore, we report that IGF-1 stimulated the nuclear translocation of P-AKT, and the transcription factors HIF-1$\alpha$ and cAMP-responsive element-binding protein (P-CREB). These nuclear events were correlated with the expression of genes that depend upon CREB and HIF-1$\alpha$. In addition, we searched the promoters of IGF-1–regulated genes in an attempt to find common molecular features that could explain why temporal

expression patterns occurred. We describe a temporal correlation between distinct transcription-binding sites and temporal gene expression regulated by IGF-1. The coupling of gene expression profiling and the analysis of promoter regulatory regions may provide insight into the underlying mechanism of how other genes in the cluster are induced or repressed.

## Materials and Methods

### *Cell Lines*

The 184htert cell line was created by the introduction of a retrovirus expressing the human telomerase reverse transcriptase gene into normal breast epithelial cells (184) obtained from Dr. Martha Stampfer. We maintained the 184htert (generous gift from Dr. Toshi Tahara) in MEMB (Clonetics, Walkersville, MD) supplemented with Single Quots (Clonetics, San Diego, CA), transferrin (Sigma, St. Louis, MO), isoproterenol (Sigma), and 400 $\mu$g/ml G418 in 2% $CO_2$. All of the other cell lines were purchased from American Type Culture Collection (Rockville, MD) and maintained in 10% fetal calf serum, DMEM F12 in 5% $CO_2$. The PI3K inhibitor, LY294002, and all other chemicals were purchased from Sigma. IGF-1 (des-IGF-1; GroPep, Adelaide, Australia) was added at a concentration of 100 ng/ml in serum-free DMEM F12. The responsiveness of the 184htrt cells to IGF-1 was confirmed by cell growth assays (communicated by Dr. Michael Pollak, McGill University). Furthermore, we observed that the cells did not undergo apoptosis following the withdrawal of serum over a 24-hour period (data not shown). There was no evidence of cells detaching from the plate or changes in cellular morphology.

### *Microarray Hybridizations and Analyses*

The 184htert cells ($1\times10^8$/150 mm dish) were treated without or with IGF-1 for 2, 4, 6, and 24 hours. The plating density was selected so that the cells were 95% to 100% confluent. The RNA was isolated using Qiagen Midi Kit (Qiagen, Valencia, CA). Detailed protocols for microarray methods and procedures are available at the website http://dir.niehs.nih.gov/microarray. Briefly, total RNA was isolated from each sample with a Qiagen Midi Kit. An in-house–generated cDNA microarray chip (Toxchip v 1.0) was used for gene expression profiling experiments [34]. A complete listing of the genes on this chip is available at this website, http://dir.niehs.nih.gov/microarray/chips.htm. cDNA microarray chips were prepared according to DeRisi et al. [35]. The spotted cDNA were derived from IMAGE clones that covered the 3′ end of the gene and ranged in size from 500 to 2000 bp. M13 primers were used to amplify insert cDNA from purified plasmid DNA in a 100-$\mu$l polymerase chain reaction (PCR) reaction mixture. A sample of the PCR products (10 $\mu$l) was separated on 2% agarose gels to ensure quality of the amplifications. The remaining PCR products were purified by ethanol precipitation, resuspended in ArrayIt buffer (Telechem, San Jose CA), and spotted onto poly-L-lysine–coated glass slides using a modified, robotic DNA arrayer (Beecher Instruments, Bethesda MD). Total RNA (35 $\mu$g) was labeled with Cy3- and Cy5-conjugated dUTP (Amersham, Piscataway, NJ) by reverse transcription (RT) reaction and hybridized to the cDNA microarray. Each RNA pair was hybridized to a total of three arrays with a fluor reversal, meaning that for one array the control was labeled with the Cy3 dye, and for two arrays it was labeled with Cy5. The same RNA source was used for each of the replicates. The cDNA chips were scanned using an Axon Scanner (Axon Instruments, Foster City CA). A custom script has been implemented in the Axon software to allow autobalancing of the two channels. The raw pixel intensity images were analyzed using the ArraySuite v1.3 extensions of the IPLab image processing software package (Scanalytics, Fairfax, VA). This program uses methods that were developed and previously described by Chen et al. [36] to locate targets on the array, measure local background for each target and subtract it from the target intensity value, and to identify differentially expressed genes using a probability-based method. We have previously determined that significant autofluorescence of the gene features on the array, attributed to spotting solution, occurs at high scanning power. We measured the pixel intensity level of "blank" spots comprised of spotting solution. The data were then filtered to provide a cut off at the intensity level just above the blank measurement values to remove from further analyses those genes having one or more intensity values in the background range. After pixel intensity determination and background subtraction, the ratio of the intensity of the IGF-stimulated cells to the intensity of the control was calculated. The ratio intensity data from a panel of 72 control genes (list available at http://dir.niehs.nih.gov/microarray/datasets) were used to fit a probability distribution to the ratio intensity values and estimate the normalization constants ($m$ and $c$) that this distribution provides. The constant, $m$, which provides a measure of the intensity gain between the two channels, ranged from 0.8 to 1.2 for all arrays, indicating that the channels were approximately balanced near a value of 1.0. For each array, the ratio intensity values were normalized to account for the imbalance between the two fluorescent dyes by multiplying the ratio intensity value by $m$. The other constant, $c$, estimates the coefficient of variation for the intensity values of the two samples. All arrays in this analysis had a $c$ value of 0.2 or less. The probability distribution that is fit to the data was used to calculate a 95% confidence interval for the ratio intensity values. Genes having normalized ratio intensity values outside of this interval were considered to be differentially expressed. The list of differentially expressed genes at the 95% confidence level was created and deposited into the NIEHS MAPS database [37]. Genes were only submitted to the list if they were differentially expressed in at least two of three replicate experiments. Any of these genes that indicated fluor bias or high variation were not considered for further analysis. Assuming that the replicate hybridizations are independent, a calculation using the binomial probability distribution indicated that the probability of a single gene appearing on this list when there was no real differential expression is

approximately 0.007. Finally, hierarchical cluster analysis was carried out with the Cluster/TreeView package [38] to group genes by the similarity of their gene expression changes over time. The data were also analyzed using GeneSpring (Silicon Genetics, Redwood City, CA) to examine gene expression profiles across time and to identify clusters of genes that exhibit similar expression patterns. The entire dataset is available at the website http://dir.niehs.nih.gov/microarray/datasets. The numbers next to the gene name are the corresponding IMAGE consortium clone identification number.

To assess the stability of gene expression for the control cells, the pixel intensity values for the control samples were compiled from each array. After transforming to the $\log_2$ scale, each value was standardized using the mean and standard deviation of all log intensity values on that array. Averaging the standardized log intensities for replicates gave a $1920\times4$ matrix of values, where the rows represent all genes on the array and the columns represent the four time points. The similarity of the controls at the four time points can be measured by considering the correlation of the averaged log intensity values for the four times. The column of values for the 2-hour time point was compared to each of the other times using Pearson correlation, and the results were as follows:

| Time points compared | Pearson correlation |
|---|---|
| 2 hours/4 hours | 0.9271 |
| 2 hours/6 hours | 0.9389 |
| 2 hours/24 hours | 0.9209 |

These correlation coefficients indicate that there is good agreement between the control intensities at 2 hours and each of the subsequent times.

*Protein and mRNA Validations*

*Real-Time Fluorogenic RT-PCR (TaqMan)* The 184htert cells ($1\times10^8$/150 mm dish) were treated without or with IGF-1 for 0, 0.5, 1, 2, 4, 6, 8, and 24 hours and the RNA was isolated as described above. RNA was then reverse-transcribed in a 9600 GeneAmp PCR system using a TaqMan Reverse Transcription Reagents Kit (Perkin-Elmer Applied Biosystems, Foster City, CA). $VEGF_{165}$ primers and probes were chosen using Primer Express Software (Perkin-Elmer Applied Biosystems).

**Primers and Probe for $VEGF_{165}$**
Forward primer: 5′-TGTGAATGCAGACCAAAGAAAGAT-3′.
Reverse primer: 5′-TCAGAGCGGAGAAAGCATTTG T-3′.
Probe: 5′-AGCAAGACAAGAAAATCCCTGTGGGCC-3′.

$VEGF_{165}$ primers (300 nM), $VEGF_{165}$ fluorogenic dual-labeled probe (100 nM), 10-$\mu$l aliquots of cDNA sample, and $2\times$ TaqMan Universal PCR Reaction Mix were added together, yielding a reaction volume of 50 $\mu$l. Amplification was carried out in an ABI Prism 7700 Sequence Detector. To degrade any contaminating genomic DNA, the AmpErase UNG enzyme was activated at 50°C/2 min. The samples were then subjected to a hotstart, 95°C/10 min followed by denaturation 95°C/15 sec, then annealing and extension was carried out at 60°C/1 min for a total of 40 cycles. TATA box-binding protein (TBP) mRNA was measured as a housekeeping gene according to the recommended protocol for this predeveloped assay reagent (PDAR; Perkin-Elmer Applied Biosystems). Quantification of c-*fos*, *IL-1B*, *fas ligand*, *cyp 1A1*, and *cyp1B1* was performed using PDARs. Each data point was replicated four times. The data were analyzed by comparing the threshold cycle number or $C_t$. A lower $C_t$ value indicates more template mRNA in the sample. The $C_t$ values were normalized by subtracting target gene $C_t$ values from the TBP $C_t$ values. The resulting numbers were taken to the exponent of 2, to reflect the fact that PCR doubles the amount of template every cycle.

*VEGF and urokinase plasminogen activator (uPA) Protein Determinations*

The 184htert, MDA-MB-231, MDA-MB-436, MDA-MB-435, MDA-MB-453, BT474, Hs578T, MDA-MB-175, MDA-MB-157, and HBL100 cells were plated at a density of $5\times10^4$ in a 96-well dish. Prior to exposure to IGF-1, they were rinsed with PBS and serum-starved for 24 hours. The conditioned medium was collected from IGF-1 treated and untreated cells for 24 hours and stored at −80°C. The $VEGF_{165}$ ELISA assay was performed according to the manufacturer's instructions (R&D Systems, Minneapolis, MN), except that the conditioned medium was not diluted. uPA protein in the conditioned media taken from the 184htert cells was measured using a commercially available kit (American Diagnostica, Greenwich, CT) previously described [39].

*Western Blots*

The 184htert cells ($1\times10^8$/150 mm dish) were plated in T150 culture flasks. The following day, the cells were rinsed with PBS and placed in serum-free DMEM F12 for 24 hours. The next day, cells were treated without or with IGF-1 at 2, 4, 6, and 24 hours. These were the same conditions used to treat the cells for RNA isolations. We also used the same passage number for protein and RNA analyses. Cells were harvested by scraping and homogenizing in four packed cell volumes of ice-cold lysis buffer [10 mM HEPES (pH 7.9), 1.5 mM $MgCl_2$, 10 mM KCl, 1 mM EDTA, 0.1% NP-40, 0.5 mM DDT, 1 mM $Na_3VO_4$, 20 $\mu$g/ml aprotinin, 2 $\mu$g/ml leupeptin, 2 $\mu$g/ml pepstatin, 1 mM NaF, 400 $\mu$M (4-amidinophenyl)-methanesulfonyl fluoride (APMSF)]. The cell lysates were centrifuged at 10,000*g* for 2 minutes at 4°C and the resulting cytoplasmic extracts were snap-frozen in liquid nitrogen and stored at −80°C. The pellets were resuspended in one PCV of nuclear lysis buffer [0.42 M NaCl, 20 mM HEPES (pH 7.9), 1.5 mM $MgCl_2$, 0.5 mM DTT, 400 $\mu$M APMSF, 2 $\mu$g/ml leupeptin, 2 $\mu$g/ml pepstatin, 2 $\mu$g/ml aprotinin, 1 mM $NaVo_4$, 1 mM NaF], and mixed every 10 minutes for a total of 40 minutes. Nuclear debris was removed by centrifugation at 14,000*g* for 10 minutes at 4°C. Extracts were snap-frozen in liquid nitrogen and stored at

−80°C until analyses were performed. Western blot analysis was performed as previously described [21] with the exception of the following modifications. P-AKT, P-CREB, and CREB were detected by polyclonal antibodies according to the manufacturer's instructions (New England Biolaboratories, Beverly, MA). The HIF-1$\alpha$ antibody (OZ12 clone) was purchased from Neomarkers (Freemont, CA).

*In Silico Promoter Analyses*

We used a collection of public databases to find transcription factor-binding sites. These databases included the transcription regulatory regions database (www.mgs.bionet.nsc.ru/mgs/dbases/trrd4/), eukaryotic promoter database (www.epd.isb-sib.ch), pubmed and genebank provided through the National Center for Biotechnology Information (www.ncbi.nlm.nih.gov). The MatInspector (http://genomatix.gsf.de/) was queried for query promoters that were not previously mapped.

## Results

*Profiling of Genes Differentially Expressed by IGF-1*

Differential gene expression was evaluated by comparing 184htert cells treated with or without IGF-1 for 2, 4, 6, and 24 hours using cDNA microarray. We found 156 (8%) of the known genes and 24 (1.2%) expressed sequence tags (ESTs) changed out of a total of 1920 with IGF-1 treatment. The genes were categorized into six functional groups: cancer progression, transcription factors, cell cycle, signal transduction, extracellular matrix, and metabolism (Table 1). We found it intriguing that IGF-1 regulated many genes involved in cancer progression. A remarkable number of the genes have defined roles in angiogenesis (Table 1); genes indicated in bold). The significance of changes in genes related to angiogenesis is discussed below. Additional details of the genes that are differentially regulated by IGF-1 can be viewed at http://dir.niehs.nih.gov/microarray/datasets/. IGF-1 also differentially regulated several genes important for cell growth and the inhibition of apoptosis. The complex regulation of cell growth was exemplified by the fact that IGF-1 stimulated the expression of cell cycle genes that promote proliferation (*cyclin-dependent kinase 7* and *notch 4*). IGF-1 also downregulated genes that suppress cell growth such as *ephrin-1A* and *wee-1*. The regulation of genes involved in apoptosis was similarly complex where IGF-1 induced genes that prevent apoptosis (*peripheral type benzodiazepine receptor* and *myeloid leukemia cell differentiation protein, MCL-1*) and suppressed genes that promote apoptosis (*fas ligand*, *FAST kinase*, *cytochrome c oxidase*, and *BCL-2 interacting killer*). We also noticed that several genes were differentially regulated at multiple time points, thus providing evidence for sustained regulation. For example, fas ligand was negatively regulated at the 2-, 6-, and 24-hour time points. There were also cases where a different portion of the same gene was spotted on the chip as indicated by different accession numbers. In all of the cases, hybridization occurred in both cDNA and the relative effect of IGF-1 on the expression of the gene was the same, e.g., *BCL-2 interacting killer*, *fas ligand*, *PTEN*, *Jun B*, *insulin-induced protein-1*, and *Metallothionein*, thus providing cross-validation of the microarray process. The summation of these results suggests that IGF-1 signaling has a broad influence on many cellular processes that could contribute to cancer progression.

We confirmed the expression of c-*fos*, *VEGF*, *IL1B*, *cyp1A1*, *cyp1B1*, and *fas ligand* by TaqMan analyses at 0, 1, 2, 4, 6, 8, and 24 hours because these genes are reported to be involved in cancer progression. Additional time points were added to further define the regulation of these genes by IGF-1. The induction of c-*fos* mRNA by IGF-1 at the 2-hour exposure was confirmed by TaqMan. Both techniques revealed a three-fold induction, while the additional time point at 1 hour showed an 11-fold induction of c-*fos* mRNA by IGF-1 (Figure 2*A*). The quantification of genes repressed by IGF-1 (*cyp1A1*, *cyp1B1*, and *fas ligand*) by TaqMan was consistent with the relative changes in mRNA found by microarray (Figure 2*B*). A probe for the $VEGF_{165}$ splice variant was used to expand our initial observation that IGF-1 induced VEGF mRNA by microarray analysis. The $VEGF_{165}$ splice variant was selected because it positively regulates angiogenesis in breast tumor xenografts [40]. We found that using TaqMan, $VEGF_{165}$ mRNA was induced 3.0-, 7.8-, 5.8-, 6.6-, and 5.9-fold at 1, 2, 4, 6, and 8 hours, respectively (Figure 2*A*). In addition, induction of the $VEGF_{165}$ protein by IGF-1 was confirmed in the conditioned media taken from 184htert cells treated with IGF-1 for 0, 2, 4, 6, and 24 hours (data not shown). To further support these findings, a panel of breast cancer cell lines was screened for the induction of $VEGF_{165}$ protein by IGF-1. The induction of $VEGF_{165}$ protein was relatively widespread, with the most notable changes occurring in the highly malignant cell lines MDA-MB-231, MBA-MB-435, and Hs578T (Figure 2*C*). Finally, we validated the induction of uPA protein by ELISA. There was approximately four-fold more uPA protein in the conditioned media from cells treated with IGF-1 compared to the untreated controls after 24 hours (data not shown). These data are in support of a previous study where IGF-1 induced uPA in breast cancer cells [39].

*Temporal Profiling of Nuclear Proteins Following IGF-1 Treatment*

In addition to characterizing genes that are differentially regulated by IGF-1, we followed a signal transduction pathway connecting the cytoplasm to the nucleus. We chose the PI3K/AKT pathway because of our interest in the role of AKT in mediating gene expression. Treatment of 184htert cells with IGF-1 resulted in the nuclear translocation of P-AKT protein at 2, 4, 6, and 24 hours (Figure 3*A*). The sustained activation of P-AKT correlated with the regulation of several genes that are known to be dependent upon the PI3K/AKT pathway. Some of the genes regulated by AKT include: *peripheral benzodiazepine receptor*, *cyclooxygenase-2*, *fas ligand*, *breast carcinoma fatty acid synthase*, *v-myc*, *uPA*, *VEGF*, *myeloid cell leukemia-1*, and *L-myc* (see

**Table 1.** The Effect of IGF-1 on Gene Expression.

| GenBank | Description | Time (hr) | Mean ratio |
|---|---|---|---|
| *Cancer progression* | | | |
| N70825 | Amphiphysin (Stiff-Mann syndrome in breast cancer) | 6 | 2.49 |
| | BCL2-interacting killer | 2 | 1.09 |
| AA576942 | BCL2-interacting killer | 2 | 1.06 |
| H12940 | Breast carcinoma fatty acid synthase | 2, 4, 6 | 0.67, 0.54, 0.56 |
| AA044993 | Connective tissue growth factor (IGFBP-8) | 24 | 0.47 |
| R80217 | Cyclooxygenase 2 (hCox 2) gene | 2 | 1.73 |
| AA045731 | Early growth response protein-1, TGFB-inducible | 2 | 1.93 |
| AA081126 | Ephrin A1 tyrosine kinase ligand | 2, 4, 6 | 0.61, 0.46, 0.50 |
| AA494493 | Fas ligand; TNF ligand | 2, 24 | 1.13, 0.660 |
| AA477173 | Fas ligand; TNF ligand | 6 | 0.54 |
| R89170 | Focal adhesion kinase | 2, 4, 6, 24 | 0.71, 0.39, 0.46, 0.55 |
| R20750 | FOS oncogene | 2, 24 | 3.02, 0.56 |
| W81586 | Gardner-Rasheed feline sarcoma viral (v fgr) homolog of src2 | 4, 24 | 2.68, 5.67 |
| AA054552 | GRO1 oncogene (melanoma growth-stimulating activity, alpha) | 6 | 0.51 |
| AA057188 | GT198 | 2 | 1.59 |
| N98757 | Hepatic angiopoietin-related protein | 2 | 1.43 |
| W46413 | Inhibitor of DNA binding-3 | 2 | 1.50 |
| AA040602 | Insulin-like growth factor binding protein-3 | 2 | 0.71 |
| R50354 | Leukemia inhibitory factor (cholinergic differentiation factor) | 2, 24 | 2.24, 0.46 |
| W47073 | Leukemia virus receptor 1 (GLVR1) | 2, 4 | 1.92, 1.92 |
| W49497 | MMP 1 (interstitial collagenase) | 4, 6 | 3.42, 1.9 |
| AA079861 | MMP 9 (gelatinase B) | 4 | 2.32 |
| AA017648 | MCL1 (myeloid leukemia cell differ protein) | 2 | 1.59 |
| T84055 | Ovarian cancer downregulated myosin heavy chain homolog (Doc1) | 2 | 1.87 |
| AA056606 | Peripheral-type benzodiazapine receptor | 2, 4, 24 | 1.41, 2.09, 2.18 |
| T49159 | Plasminogen activator inhibitor, type II (arginine serpin) | 24 | 0.55 |
| N98421 | PTEN | 2 | 1.57 |
| W37864 | PTEN | 2 | 1.16 |
| N68057 | Telomeric repeat-binding factor 1 | 4, 6 | 0.51, 0.57 |
| W49722 | Tissue inhibitor of metalloproteinase 2 | 24 | 0.58 |
| T86483 | Transferrin | 4 | 2.37 |
| N47476 | Transmembrane 4 superfamily member 1 | 2, 4, 24, | 0.65, 0.49, 0.59 |
| AA487893 | Transmembrane 4 superfamily member 1 | 4, 24 | 0.49, 0.58 |
| AA115151 | Tumor-associated calcium signal transducer 2 | 6, 24 | 0.58, 0.52 |
| AA040727 | uPA | 2, 6, 24 | 1.51, 0.55, 0.53 |
| AA148025 | uPA receptor | 2, 24 | 1.85, 0.60 |
| W87741 | v-myc avian oncogene | 2, 6 | 1.99, 1.78 |
| W19225 | Vascular endothelial growth factor | 2 | 1.53 |
| R62813 | v-myc 1 | 2, 4 | 0.64, 0.51 |
| T87495 | Zinc alpha-2 glycoprotein; ZAG | 2 | 1.48 |
| *Transcription factors* | | | |
| AA053239 | A20 DNA-binding protein, NFKB inhibitor | 2 | 1.64 |
| W87473 | CCAAT box-binding transcription factor 1 | 6 | 1.61 |
| AA004524 | Cleavage and polyadenylation spec factor, 160-kDa subunit | 4 | 1.88 |
| W46792 | DP2 (Humdp2) | 24 | 1.81 |
| T89996 | Fos-related antigen 1 (fra1) | 2 | 2.54 |
| H91734 | GA-binding protein transcription factor, beta subunit 1 (53 kDa) | 4 | 1.91 |
| R31442 | GATA-binding protein 3 | 2 | 0.62 |
| AA503220 | Jun B | 2 | 2.08 |
| W46228 | Jun B | 2 | 1.81 |
| R41791 | LIM domain kinase 1 | 2, 4 | 0.96, 2.26 |
| R77770 | Nuclear receptor coactivator 2 | 4 | 0.50 |
| AA046245 | Osteoblast-specific factor 2 (OSF 2p1) | 2, 4, 6 | 0.62, 0.45, 0.53 |
| AA011627 | POU domain, transcription factor 2 | 2 | 1.60 |
| AA115165 | Stat 3 | 2 | 1.15 |
| W95433 | Steroid hormone receptor, NER | 4 | 2.04 |
| W70150 | SW1/SNF–related chromatin regulator | 24 | 1.73 |
| H83548 | Transcription elongation factor B (SIII), elongin A | 24 | 0.48 |
| W45393 | Transcription factor ATF 7 | 4 | 1.98 |
| R67075 | Zinc finger protein, (ZFX putative transcription activator) | 2, 4 | 1.07, 1.32 |
| AA043478 | Zinc finger protein, homologous to mouse Zfp 36 | 2 | 1.51 |
| *Cell cycle* | | | |
| W80586 | CDC46 homolog | 2 | 1.03 |
| AA031961 | CDK7 | 2, 4, 6 | 0.46, 0.47, 0.59 |
| N64843 | CDK inhibitor 3 | 24 | 1.71 |
| AA113188 | GADD45 B | 2, 4, 6 | 0.67, 0.47, 0.61 |
| | Notch 4 | 2 | 1.90 |

*(continued on next page)*

**Table 1.** (*continued*)

| GenBank | Description | Time (hr) | Mean ratio |
|---|---|---|---|
| AA740551 | PMS4 homolog mismatch repair protein | 2 | 1.21 |
| AA026057 | Thyroid autoantigen 70 kDa (ATP-dependent DNA helicase II) | 24 | 2.72 |
| AA039640 | WEE1-like tyrosine kinase | 2, 4 | 0.33, 0.45 |
| *Signal transduction* | | | |
| H43049 | Activin receptor-like kinase 1 | 4 | 2.24 |
| AA045331 | ADP ribosylation factor 4-like, G-protein coupled | 2 | 1.74 |
| AA143571 | cAMP-dependent protein kinase, type 1, alpha | 2 | 1.31 |
| R78286 | CD94 antigen; killer cell lectin-like receptor | 2 | 1.14 |
| N70450 | Coagulation factor II (thrombin) receptor | 6 | 0.50 |
| T79330 | Complement factor H-related gene 3 | 2 | 1.42 |
| W49546 | Cytokine-inducible kinase | 2 | 2.19 |
| W19215 | Decay accelerating factor for complement (CD55) | 4 | 0.48 |
| W65461 | Dual specificity phosphatase 5 | 2 | 1.77 |
| AA056608 | Dual specificity phosphatase 10 | 2 | 0.70 |
| W72792 | Ephrin receptor, EphB2 | 2 | 1.66 |
| AA074202 | Epidermal growth factor receptor substrate 15 | 2 | 1.14 |
| R84974 | Fibroblast growth factor receptor 3 | 24 | 1.87 |
| AA045013 | G protein alpha-inhibiting activity polypeptide 2 | 2, 6 | 0.66, 0.61 |
| R25530 | GABA A receptor, Alpha 1 | 2 | 1.09 |
| R35346 | GABA A receptor, Alpha 5 | 2 | 1.12 |
| H63532 | GABA A receptor, epsilon subunit | 2 | 0.67 |
| AA053124 | Heparin-binding EGF-like growth factor | 2 | 2.40 |
| AA084517 | HSP40 homolog | 2 | 0.55 |
| AA046719 | Insulin-induced gene 1; INSIG1 | 2, 4 | 1.64, 2.11 |
| AA007569 | Insulin induced gene -1; INSIG1 | 2 | 1.97 |
| R39575 | Interleukin 1 receptor, type II | 4 | 3.02 |
| W47225 | Interleukin 1, beta | 2, 4 | 2.21, 1.97 |
| H43839 | Latent transforming growth factor beta binding protein 2 | 24 | 0.60 |
| AA055059 | MacMarcks | 24 | 0.58 |
| AA034481 | Mannose-6-phosphate receptor | 2 | 0.69 |
| R59864 | MAP kinase phosphatase 3; DUSP6 | 2 | 2.18 |
| AA055467 | Ornithine decarboxylase 1 | 2 | 1.39 |
| R15351 | Protein kinase C binding protein | 2 | 0.67 |
| AA005215 | Protein kinase C delta | 2 | 1.41 |
| H84974 | Protein kinase, cAMP -dependent, regulatory, type II, beta | 6, 24 | 1.70, 2.28 |
| N50894 | Protein tyrosine phosphatase, receptor type, Z polypeptide 1 | 6 | 1.71 |
| AA047066 | PTEN-induced putative kinase 1 | 6 | 0.59 |
| N23875 | Serine/threonine protein kinase 4; Krs2 | 4, 6 | 1.93, 1.75 |
| N77456 | Serum/glucocorticoid–regulated kinase; SGK | 2, 6 | 0.58, 0.56 |
| N56944 | Thioredoxin reductase I | 2, 6 | 0.70, 0.56 |
| AA187644 | Thioredoxin reductase I | 6 | 0.58 |
| H51007 | Tyrosine phosphatase (IA 2/PTP) | 24 | 1.92 |
| R07707 | Tyrosine phosphatase nonreceptor-type, 1 | 2, 4, 6, 24 | 1.96, 2.54, 1.92, 1.83 |
| AA053973 | Ubiquitin conjugating enzyme (E2B) | 6 | 0.55 |
| *Extracellular matrix* | | | |
| AA100382 | Amyloid beta (A4) precursor protein | 2, 6 | 1.03, 1.17 |
| H44575 | BPAG1 (plectin) | 2, 4, 6 | 0.62, 0.52, 0.51 |
| R54968 | Collagen, type XVI, alpha 1 | 2, 4, 6, 24 | 1.68, 2.34, 2.13, 2.03 |
| AA159273 | Collagen, type VII, alpha | 6 | 0.53 |
| AA069027 | Integrin, alpha 2 (CD49B, alpha 2 subunit of VLA 2 receptor) | 6 | 0.52 |
| AA001432 | Laminin alpha 3 (LamA3) | 24 | 0.49 |
| AA076664 | Laminin, beta 3 (nicein (125 kDa), kalinin (140 kDa) | 24 | 0.63 |
| AA055478 | Laminin, alpha 4 | 4 | 2.50 |
| AA055637 | S100A2 | 6 | 0.59 |
| *Metabolism* | | | |
| AA040600 | AMP-activated protein kinase, gamma 1 subunit | 6, 24 | 0.59, 0.28 |
| AA054748 | Aldehyde dehydrogenase 6 | 24 | 0.38 |
| W79785 | Aldehyde dehydrogenase 8 | 24 | 2.57 |
| T62755 | Apolipoprotein A 1 precursor; APOA1 | 4 | 0.54 |
| R63185 | Apolipoprotein E receptor 2 | 4, 6 | 2.20, 1.60 |
| | Corticosteroid binding globulin | 24 | 1.70 |
| AA418907 | Cytochrome P450 IA1 | 4 | 0.43 |
| N98684 | Cytochrome c oxidase subunit VIc | 24 | 0.61 |
| AA040872 | Cytochrome P450 IB1 (dioxin inducible) | 4, 6 | 0.44, 0.54 |
| H05935 | Cytochrome P450, subfamily XXVII A | 2, 4, 6 | 1.72, 1.24, 1.28 |
| AA574223 | Glutathione reductase | 2 | 1.15 |

*(continued on next page)*

**Table 1.** (*continued*)

| GenBank | Description | Time (hr) | Mean ratio |
|---|---|---|---|
| H65189 | Glycogen synthase kinase-3beta; GSK3B | 4 | 2.28 |
| AA004597 | Heat shock protein 70 related protein | 6 | 1.70 |
| AA043817 | Leptin receptor | 2, 24 | 1.48, 0.54 |
| T74249 | Leptin receptor | 6 | 0.60 |
| T68228 | Low density lipoprotein receptor-related protein 6 | 2 | 1.69 |
| AA037443 | Metallothionein 2A | 6 | 0.55 |
| W73203 | Metallothionein 1e gene (MT 1e) | 6 | 0.56 |
| H77597 | Metallothionein 1H | 6 | 0.60 |
| N77931 | N-acetylglucosaminidase, alpha (Sanfilippo disease IIIB) | 6 | 0.55 |
| H25860 | NAD(P)H dehydrogenase | 24 | 1.68 |
| AA025552 | NADPH flavin reductase | 6 | 0.60 |
| AA046316 | Phospholipid hydroperoxide; glutathione peroxidase 4 | 2, 6 | 0.68, 0.50 |
| H84974 | Protein kinase, cAMP dependent, regulatory, type II, beta | 4 | 2.52 |
| H25590 | Serum amyloid protein precursor | 4, 24 | 0.53, 0.56 |
| W45418 | S-adenosylmethionine decarboxylase | 4 | 1.86 |
| H11561 | Thioredoxin reductase 1 | 4, 6 | 0.6, 0.52 |
| *EST and others* | | | |
| | EST | 2 | 1.26 |
| T90376 | EST | 2, 6 | 1.61, 1.09 |
| W73510 | EST | 4 | 0.49 |
| AA058510 | EST | 4 | 0.55 |
| R10161 | EST | 4 | 2.09 |
| AA010416 | EST | 4, 24 | 0.64, 0.57 |
| AA039870 | EST | 6 | 2.13 |
| W84634 | EST | 4 | 1.91 |
| H79617 | Est | 2, 4, 6 | 0.69, 0.55, 0.53 |
| R83223 | EST | 4 | 1.32 |
| AA058704 | EST similar to MAP kinase phosphatase I | 6 | 0.62 |
| R97218 | EST similar to TVHUME | 2, 4 | 1.09, 1.35 |
| R39317 | EST similar to tyrosine kinase receptor, ephrin B3 | 2 | 1.62 |
| | EST, clone ID 530030 | 6 | 1.33 |
| H98630 | EST, hypothetical protein FLJ20287 | 6 | 1.69 |
| T66824 | EST, similar to complement C3b/C4b receptor-like precursor | 6 | 1.67 |
| AA081098 | EST, similar to GA binding protein beta 2 chain | 2 | 1.05 |
| H73129 | EST, similar to p300/CBP | 4 | 3.26 |
| W85846 | EST, similar to IL1 receptor accessory protein precursor | 2, 6 | 1.83, 2.00 |
| W24201 | ESTs similar to ROS1 oncogene | 6 | 1.70 |
| R01478 | ESTs, moderately similar to I78855 serine/threonine–specific protein kinase | 4, 24 | 2.12, 1.94 |
| | Histone deacetylase 3 | 2 | 1.68 |
| N47581 | Imprinted in Prader-Willi syndrome | 2 | 1.17 |
| AA044722 | Signal sequence receptor, beta | 2 | 1.54 |
| R79560 | Tight junction protein 1 (zona occludens 1) | 2, 4 | 1.52, 1.44 |
| AA035626 | Vacuolar sorting protein 33B | 6 | 0.61 |

Microarray analysis of genes differentially expressed in the presence of IGF-1 at 2, 4, 6, and 24 hours. The genes that were differentially expressed were organized into functional groups: cancer progression, transcription factors, cell cycle, signal transduction, extracellular matrix, and metabolism. Several expressed sequence tags were also differentially regulated by IGF-1. In an effort to focus on some of the salient features of our microarray results, only the genes involved in cancer progression are illustrated. It was noted that several genes in this functional group are also linked to angiogenesis (bold). The entire gene list is available as supplemental material (www.pnas.org). The mean calculated ratios were only presented if they were considered statistically significant (details in the Materials and Methods section).

Table 1) for temporal comparisons). It was noted that these genes were differentially expressed throughout the 24-hour time course and these data correlated with the presence of P-AKT in the nucleus. These data provide a temporal association between P-AKT and gene expression. Next, we investigated the relationship between stimulation of the nuclear transcription factors, HIF-1$\alpha$ and P-CREB, because these transcription factors regulate some of the genes validated above, e.g., c-*fos*, *cyp1A1*, *cyp1B1*, and *VEGF*. We found that IGF-1 stimulated the translocation of HIF-1$\alpha$ into the nucleus at the 4- and 6-hour time points (Figure 3*B*). These data were compared to genes with known HIF-1$\alpha$–responsive elements (HRE) in their promoter regions. There was a general trend toward the presence of HIF-1$\alpha$ and the regulation of genes with an HRE (*VEGF*, *transferrin*, *thioredoxin reductase*, *cyp1A1*, and *cyp1B1*). The genes with an HRE were induced at the 4- and 6- hour time points (see Table 1), although $VEGF_{165}$ was an exception to this generalization. Instead, we found that the temporal profiling of VEGF and HIF-1$\alpha$ was not coordinately regulated by IGF-1 in this model system. This point is illustrated by the fact that $VEGF_{165}$ was induced much earlier than could not be accounted for by the presence of HIF-1$\alpha$. The TaqMan data showed that VEGF mRNA was induced by three-fold in the first hour of exposure to IGF-1 (Figure 2*A*). Therefore, we suspected that other transcription factors such as CREB may be responsible for the early induction of VEGF by IGF-1. This is possible because CREB not only binds to CRE sites but it also has an affinity for HRE [41] and AP-1 consensus sequences [42]. To test this hypothesis, we followed CREB

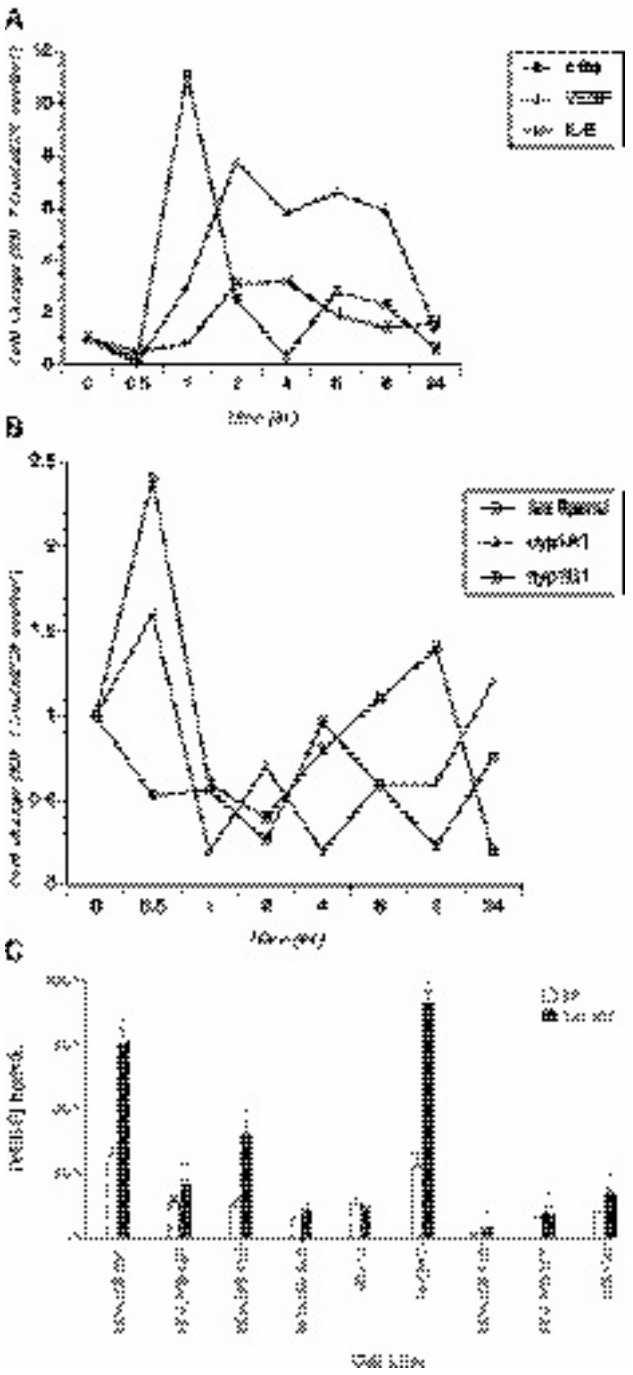

**Figure 2.** *(A) The differential expression of genes involved in cancer progression. Gene expression c-fos, VEGF-IL1B fas ligand, cyp1A1 and cyp1B1 was measured by TaqMan after 0, 0.5, 1, 2, 4, 6, 8, and 24 hours in the absence or presence of IGF-1. Each time point was replicated four times and the target gene expression was normalized to the TBP and A represents ones that were induced by IGFI while panel B illustrates repression. (C) Induction of $VEGF_{165}$ protein by IGF-1 measured in a panel of breast cancer cell lines. $VEGF_{165}$ protein was measured in breast cancer cells serum-free (SF) or with des-IGF-1. The conditioned medium was collected from each of the cell lines 24 hours after the addition media containing or des-IGF-1. *Indicates that there was a significant difference between the SF and IGF-1 treatment for each cell line, P .05, Student's t-test.*

over time and found that IGF-1 stimulated the phosphorylation of CREB at a peak of 1 hour (Figure 3*C*). Next, we examined whether AKT was responsible for the activation of CREB. To this end, we inhibited AKT with LY294002 and showed that CREB was no longer phosphorylated in cells treated with IGF-1 for 1 hour (Figure 3*D*). Finally, we noticed that coincident with the presence of nuclear P-CREB, the majority of genes possessing a cAMP-responsive element (CRE) were also induced at the 2-hour time point (*early growth response gene-1*, *myeloid leukemia cell-1*, *uPA*, *plasminogen activator-1*, *Jun B*, *cyclooxygenase-2*, c-*myc*, and c-*fos*).

*Promoter Analysis of IGF-1–Regulated Genes*

The temporal regulation of gene expression was further investigated by an extensive *in silico* promoter analysis. We surmised that genes with similar expression profiles could be

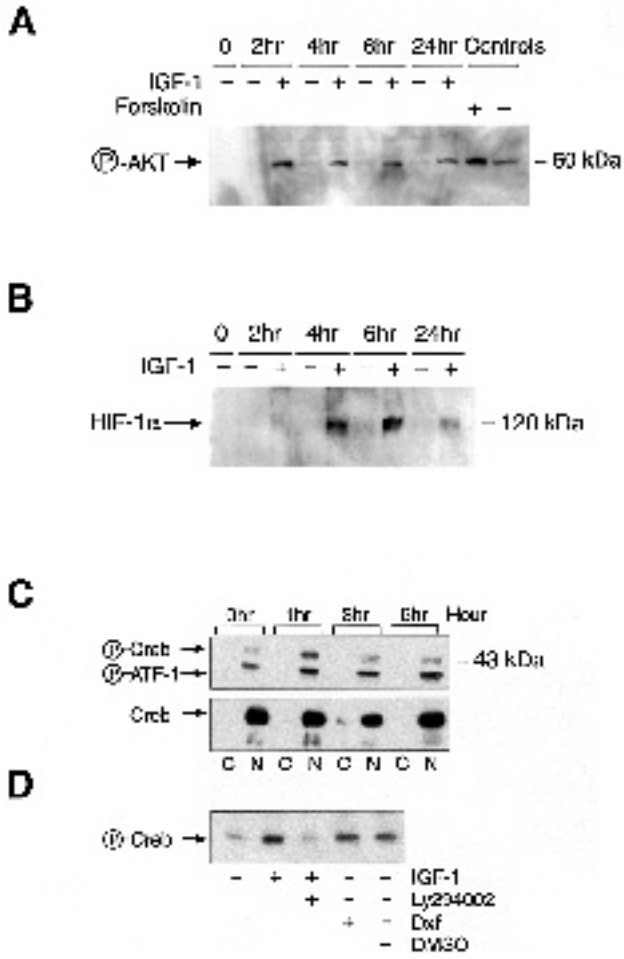


**Figure 3.** *Temporal profiling of nuclear P-AKT, HIF-1$\alpha$, and P-CREB. (A) IGF-1 stimulated the nuclear translocation of P-AKT after 2, 4, 6, and 24 hours in the 184htert cells. The controls for this experiment were SK-N-MC cells treated with forskolin (positive) and without forskolin (negative). Neither of the controls received IGF-1. (B) Temporal profiling of HIF-1$\alpha$ in the absence or presence of IGF-1. IGF-1 stimulated the translocation of HIF-1$\alpha$ at the 4- and 6-hour time points. (C) Temporal profiling of P-CREB. IGF-1 was added to the 184htert cells for 0, 1, 3, and 6 hours and the protein extracts were evaluated for P-CREB (top panel) and total CREB (bottom panel). CREB was maximally phosphorylated after 1 hour following IGF-1 treatment while there was no effect on ATF-1. The total amount of CREB protein was the same between time points (bottom panel). (D) Inhibition of AKT signal transduction with LY294002 (30 $\mu$M) inhibited the phosphorylation of CREB by IGF-1. Cells were pretreated with LY294002 for 10 minutes then IGF-1 was added for 1 hour. Desferrioxamine (DXF, 100 $\mu$M) was added to the cells for 1 hour as a positive control for p-CREB. An equal volume of dimethyl sulfoxide (DMSO) served as a vehicle control for the LY294002 compound. There was no inhibition of P-CREB in the presence of DMSO and IGF-1.*

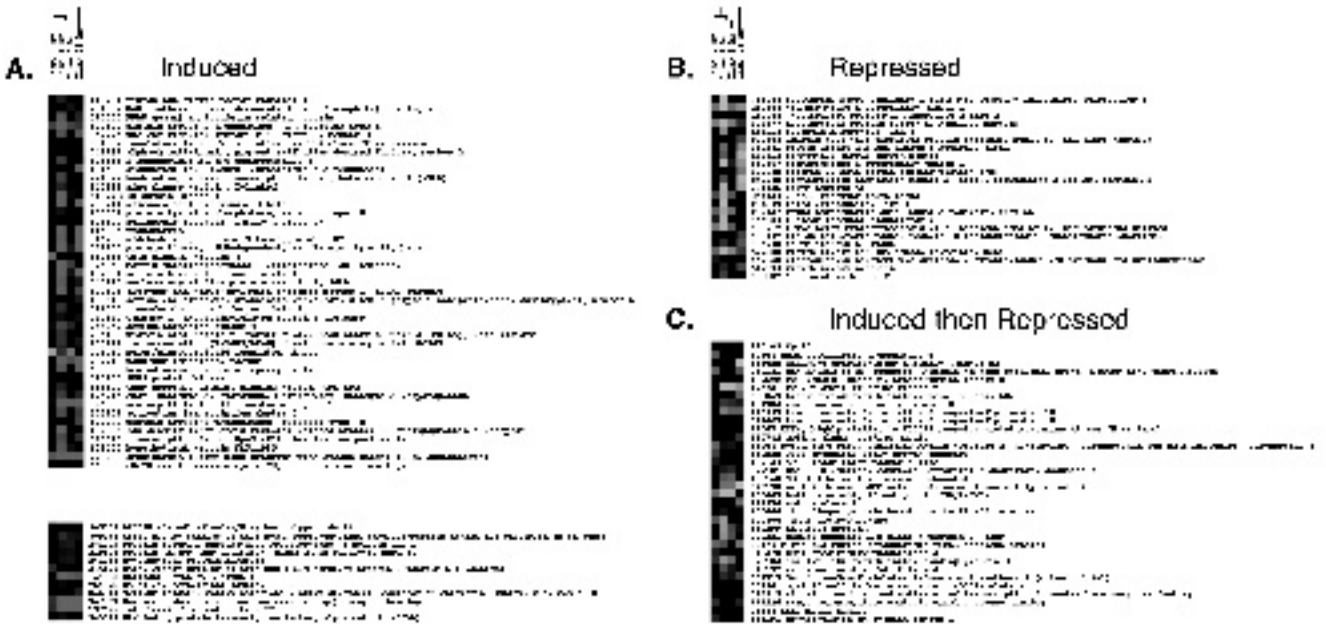


**Figure 4.** *Hierarchical clustering of genes differentially expressed at 2, 4, 6, and 24 hours. There were three major nodes found, which represent genes that were (A) induced, (B) repressed, or (C) induced then repressed. The genes that were induced were assigned a pseudo-color of red and those that were repressed were assigned a green color. The numbers next to the gene names indicate the clone identification. A complete view of the dendrogram is available at http://dir.niehs.nih.gov/microarray/datasets/.*

regulated through common regulatory sequences. The genes were organized based upon their pattern of expression by cluster analysis [38]. We noted that gene expression was clustered to the following nodes: 1) induced, 2) repressed, or 3) induced then repressed (Figure 4). Next, we searched the 5′ untranslated regions and observed that the majority of the genes that were consistently induced have CRE/AP-1/AP-2 coupled with SP-1 and ETS transcription factor-binding sites in their promoters (Table 2). In contrast, the genes that were repressed commonly had FKHR, myc, and WT-1 binding sites. These data are supported by evidence that myc negatively regulates CYP1A1 [43], GADD45 [44], and GAS [45], while WT-1 suppressed the expression of connective tissue growth factor [46]. The regulation of the genes that were transiently induced then repressed also had common regulatory regions in their promoter. Most of the genes in node C had either a CRE and/or AP-1/AP-2 binding site in the promoter. These data describe putative composite elements that are common among coordinately expressed genes.

Gene expression is commonly regulated by the transcription factors we focused upon. For example, many of the genes on the microarray have CRE or AP-1 binding sites on their promoter. What was not immediately obvious was why IGF-1 did not change their expression. To delve into this issue, we randomly selected 10 genes that were not differentially regulated by IGF-1 in our microarray experiments. The gene list was cross-referenced to http://dir.niehs.nih.gov/microarray/chips.htm to confirm that they were indeed part of the ToxChip repertoire. Then we searched the literature to determine how the genes were regulated. We also use MatInspector software by Genomatix when the promoter was not sequenced. In this case, the gene was mapped to its chromosomal location using National Center for Biotechnology Information, Map Viewer (http://www.ncbi.nlm.nih. gov/ cgi-bin/Entrez/hum_srch?chr=hum_chr.inf&query), the start site was identified, then we selected 300 bp upstream for our promoter analyses using MatInspector. We found that although the unregulated genes had common transcription factor-binding sites such as CRE and AP-1, the expression of these genes depended upon methylation or acetylation (Table 3). Furthermore, many of the genes were located in DNAse 1-hypersensitive sites, suggesting that alteration of chromatin structure is required for transcription. We summarize these data by concluding that IGF-1 induces some genes and not others based on whether or not they require methylation for expression.

## Discussion

IGF-1–responsive gene expression changes were investigated in immortalized breast epithelial cells over time. In this study, we found that 8% of the known genes and 1.2% of the ESTs were differentially regulated by IGF-1. The changes in gene expression also correlated with the presence of the nuclear proteins P-AKT, HIF-1$\alpha$, and P-CREB. An in-depth analysis of the clustering data revealed that genes that were similarly expressed had distinct transcription factor-binding sites. A similar study reported a correlation between single transcription-binding sites and gene expression in yeast [35]. Our study is the first example of coupling promoter regulation to gene expression profiles in mammalian cells. We noted that there were composite elements that characterized coordinately expressed genes. These data therefore provide a framework for understanding how some genes are regulated by

**Table 2.** Promoter Analysis of IGF-1–Regulated Genes.

| Gene | Cre | AP-1 | AP-2 | SP-1 | HIF-1 | NFkB | ETS | FKHR | EGR-1 | CCAAT | Myc | WT-1 | OCT-1 | p53 |
|---|---|---|---|---|---|---|---|---|---|---|---|---|---|---|
| *Node A: induced* | | | | | | | | | | | | | | |
| ADP ribosylation factor 4 | * | * | | * | | | * | | | | | | | |
| Aldehyde dehydrogenase | | | | * | | | | | | | | | | |
| Apoliprotein E receptor 2 | | | * | * | | | | | | | | | | |
| ATF-1 | | * | * | * | | | * | | | | | | | |
| Cyclooxygenase 2 | * | | | * | | * | * | | | | | | | |
| Cytochrome P450 XXVII | | | * | * | * | | | | | | | | | |
| Fibroblast growth factor receptor 3 | | | * | * | | | | | | | | | | |
| Heat shock protein-40 | | | | * | | | | | | | | | | |
| Heparin binding epidermal growth factor | | * | * | * | | | | | | | | | | |
| Insulin-induced protein 1 | | * | | * | | | | | | | | | | |
| Interleukin 1b | * | | | | | * | | | | | | | | |
| MMP 1 | | * | | | | | * | | | | | | | |
| MMP 2 | | * | | | | | * | | | | | | | |
| Metallothionein | | | | * | | | | | | | | | | |
| Transferrin | * | | | | * | | | | | | | | | |
| Tyrosine phosphatase 1B | | | | * | | | | | | | | | | |
| uPA | | * | | | | * | * | | | | | | | |
| uPA receptor | | * | * | * | | * | | | | | | | | |
| Vascular endothelial growth factor | | * | | * | * | | | | | | | | | |
| *Node B: repressed* | | | | | | | | | | | | | | |
| Apoliprotein A 1 precursor† | | | | * | | | | | | | | | | |
| Casein kinase 2† | | | | * | | * | | | | | | | | |
| Connective tissue growth factor | | * | | * | | | | | | | | * | | |
| Cytochrome P450 1A1 | | | | | * | | | | | | * | | | |
| Fas ligand† | | | | * | | * | | * | | | | | | |
| GADD45 | | | | | | | | | | * | * | | * | * |
| Growth arrest specific protein | | | | | | | | | | | * | | | |
| MMP-2 inhibitor† | | | | * | | | | | | | | | | |
| Serum amyloid A protein precursor | * | | | | | * | | | | | | * | | |
| *Node C: induced/repressed* | | | | | | | | | | | | | | |
| Early growth response gene-1 | * | | | | | | | | | | | | | |
| Fos related antigen-1† | | * | * | | | | | | | | | | | |
| MAP kinase phosphatase-1 | * | | | | | | | | | | | | | |
| Myeloid leukemia cell differ. protein-1 | * | | | | | | | | | | | | | |
| Plasminogen activator inhibitor I | * | * | * | | | | | | | | | | | |
| Plasminogen activator inhibitor II | * | | | | | | | | | | | | | |
| STAT3 | * | | | | | | | | | | | | | |
| V-fos | * | | | * | | | | | | | | | | |
| V-myc | * | | | | | | | | | | | | | |

†Indicates genes clustered outside of this node, but were negatively regulated by IGF-1.
*In silico* promoter analysis of IGF-1–induced genes. The 5′ untranslated region of each promoter was evaluated for transcription factor-binding site. This is a compilation of putative and experimentally validated sites. These data were compared to the clustering analysis for correlations between temporal gene expression and the presence of transcription factor-binding sites.
Additional data are available at our website, http://dir.niehs.nih.gov.microarray/datasets

IGF-1. To extend the interpretation of these data, these trends could be applied to understanding how previously uncharacterized genes are regulated. For example, the *ELKL kinase* is a serine threonine protein kinase for which the promoter has not been previously studied. *ELKL kinase* clusters with *MCL-1*, *STAT3*, and *v-myc* and these genes

**Table 3.** Regulation of Genes that were not Differentially Following IGF-1 Treatment.

| Gene | Regulation | Reference | Expression depends upon |
|---|---|---|---|
| BRCA-1 | Cre | [55] | Methylation |
| Catalase | CCAAT, ERG-1, SP-1, NF-Y | [56] | Acetylation? |
| Estrogen receptor-alpha | AP-2, CpG islands, | [57-59] | Methylation |
| Glutathione S-transferase pi | AP-1, SP-1, CpG islands | [60-62] | Methylation |
| Gycogen synthase kinase-alpha | AP-1, YY-1, LSF, MZF-1, SP-1, CRE | [63] | Unknown |
| Multidrug resistance-1 | AP-1, YB-1, CCAAT | [64,65] | Methylation |
| Topoisomerase II | CCAAT, Acetylation | [66] | Acetylation |
| Topoisomerase III | SP-1 (4), YY-1, USF-1 | [67] | Methylation |

*In silico* promoter analysis of genes that were printed on the microarray chip but not induced by IGF-1. Eight genes were randomly selected from our gene list and their promoters were queried for transcription factor-binding sites. Although many of the promoters had common transcription factor-binding sites such as CRE and AP-1, their expression depended upon methylation.

all have a CRE site in their promoters (Node C). Therefore it is reasonable to predict that this *ELKL kinase* is similarly regulated by CREB. Finally, this approach could also apply to understanding the regulation of known genes for which the promoter regulatory regions are not yet mapped. We used a combination of public databases and only found promoter regulatory maps for 36/156 of the known genes. Thus, there is still a vast gap in our knowledge of how many human genes are regulated.

Our study of the gene expression profiling of immortalized breast epithelial cells derived from the 184 parental cell line complements two previously published microarray reports that used the same parental cell line. In the first case, comparisons of gene expression were made between 184 cells and tumor cell lines by SAGE (serial analysis of gene expression) and microarray technologies [47]. In the second case, the 184 cells were used in a comparison between cell lines (normal *versus* cancer) and breast tissues (normal *versus* cancer) [33]. In both of these reports, S100A2 and bullous pemphigoid antigen (BPAG) were lost in breast cancer cell lines and tumors. Similarly, we found that IGF-1 negatively regulated S100A2 and BPAG. These reported changes could be permissive for premalignant cells to become invasive because the S100A2 protein is involved in organization of the cytoskeleton and the inhibition of cellular migration [48]. Likewise, BPAG is a protein that organizes into hemidesmisomes and connects epithelial cells to the basement membrane. Disorganization of hemidesmisomes occurs in DCIS and this cytoarchitectural feature is commonly lost in invasive breast cancer [49]. These data suggest that there is a loss of the basement membrane that could facilitate the conversion of DCIS to invasive cancers. Thus, BPAG and S100A2 are examples of genes negatively regulated by IGF-1 and are differentially expressed during cancer progression. Our data complement other gene expression databases by providing a possible mechanism for some of the observed changes. This compendium of relevant microarray databases to will inevitably enrich our understanding of breast cancer progression.

One of the goals of this study was to gain insight into potential mechanisms whereby IGF-1 relates to the risk of developing cancer. A mechanistic approach will help us to bridge the current gaps in translational research as it relates to IGF-1 and breast cancer. As an example, epidemiological studies indicate that elevated serum IGF-1 levels in premenopausal women are linked with increased mammographic density [50]. Furthermore, it is well known that high breast density is linked to a significant increase in the risk of developing breast cancer, but the biological basis for this association remains unknown. A few features of dense breasts are clear though, these tissues are characterized by an accumulation of stromal and epithelial cells. To address a possible cause for these events, it was recently shown that local tissue levels of IGF-1 and total collagen proteins are elevated in dense breast tissues [51]. We now have evidence that IGF-1 consistently induces collagen XVI at the 2-, 4-, 6-, and 24-hour time points. Given these data, we propose that endocrine and/or paracrine IGF-1 could stimulate the production of collagen XVI protein, thereby making the breast denser and masking the identification of small tumors. This is a testable hypothesis that will warrant further investigation.

IGF-1 can also contribute to the progression of cancer by promoting cell growth, inhibiting apoptosis, and stimulating invasion/metastasis. One of the conclusions that emerged from our microarray data was that IGF-1 induced many genes involved in angiogenesis. We found this of interest because angiogenesis is an essential process for the growth and metastasis of tumors [52]. The importance of angiogenesis in breast cancer progression is underscored by the fact that this process is evident in preinvasive lesions such as DCIS [53]. Several studies point toward VEGF as a potent mitogen for endothelial cells (reviewed in Ref. [54]). We found that IGF-1 induced VEGF mRNA in premalignant breast epithelial cells and in most breast cancer cell lines. Hence, IGF-1 could contribute to vascularization through VEGF, but this vascular mitogen does not stand alone as the only angiogenic factor that is important for neovascularization. We found that IGF-1 induced genes that positively regulate angiogenesis, including cyclooxygenase 2, uPA/uPAR, FGFR, transferrin, matrix metalloproteinase-1, matrix metalloproteinase-2, angiopoietin-1, interleukin B1, and the ephrin B2 receptor. In addition, many genes that inhibit angiogenesis were also repressed by IGF-1, including tissue inhibitor of matrix metalloproteinase-2, plasminogen activator inhibitor-1, plasminogen activator inhibitor-2, and protease inhibitor-1. The synchronous expression of genes that positively regulate angiogenesis suggests functional complementation. Ephrin B2 receptor and angiopoietin-1 regulate neovascularization by stimulating vessel maturation and sprouting, whereas VEGF, uPA/uPAR, and the MMPs are involved in the proliferation and migration of new blood vessels. The observation that IGF-1 regulates many different genes involved in angiogenesis necessitates finding common molecular pathways. Furthermore, understanding such pathways could lead to novel cancer intervention strategies that would inhibit classes of genes involved in angiogenesis rather than targeting single gene products. The expression profiling data and the characterization of nuclear events triggered by IGF-1 reported in this study will provide valuable insight into the regulation of cancer progression and common signal transduction pathways that control angiogenesis.

**Acknowledgements**

Our sincere gratitude is extended to Michael Pollak and Christopher Corton for their careful review of our manuscript. We also thank Tomo Oshimura, Lois Annab, and Jeff Tucker for their technical assistance in the microarray analyses.

## References

[1] Bohlke K, Cramer DW, Trichopoulos D, and Mantzoros CS (1998). Insulin-like growth factor-1 in relation to premenopausal ductal carcinoma *in situ* of the breast. *Epidemiology* **9(5)**, 570–73.

[2] Hankinson SE, Willett WC, Coldita GA, Hunter DJ, Michaud DS, Deroo

B, Rosner B, Speizer FE, and Pollak M (1998, May 9). Circulating insulin-like growth factor-1 and the risk of breast cancer. *Lancet* **351**, 1393–96.

[3] Ma J, Pollak MN, Giovannucci E, Chan JM, Tao Y, Hennekens CH, and Stampfer MJ (1999). Prospective study of colorectal cancer risk in men and plasma levels of insulin-like growth factor (IGF-1) and IGF-binding protein-3. *J Natl Cancer Inst* **91(7)**, 620–25.

[4] Yu H, Spitz MR, Mistry J, Gu J, Hong WK, and Wu X (1999). Plasma levels of insulin-like growth factor-1 and lung cancer risk: a case–control analysis. *J Natl Cancer Inst* **91(2)**, 151–56.

[5] Chan JM, Stampfer MJ, Giovannucci E, Gann PH, Ma J, Wilkinson P, Hennekens CH, and Pollak M (1998). Plasma insulin-like growth factor-1 and prostate cancer risk: a prospective study. *Science* **279**, 563–66.

[6] Yang XF, Beamer WG, Huynh H, and Pollack M (1996, April 1). Reduced growth of human breast cancer xenographs in hosts homozygous for the lit mutation. *Cancer Res* **56**, 1509–11.

[7] Dunn SE, Kari FW, French J, Leininger JR, Travlos G, Wilson R, and Barrett JC (1997). Dietary restriction reduces insulin-like growth factor-1 levels which modulates apoptosis, cell proliferation, and tumor progression in p53 deficient mice. *Cancer Res* **57**, 4667–72.

[8] Kaleko M, Rutter WG, and Miller DA (1990). Overexpression of the human insulin-like growth factor-1 receptor promotes ligand dependent neoplastic transformation. *Mol Cell Biol* **10**, 464–73.

[9] Resnicoff M, Sell C, Rubini M, Coppola D, Ambroso D, Baserga R, and Rubin R (1994). Rat glioblastoma cells expressing an antisense RNA to the insulin-like growth factor-1 receptor are nontumorigenic and induce regression of wild-type tumors. *Cancer Res* **54**, 2218–22.

[10] Shapiro DN, Jones BG, Shapiro LH, Dias P, and Houghton PJ (1994). Antisense mediated reduction in insulin-like growth factor I receptor expression suppresses the malignant phenotype of a human alveolar rhabdomyosarcoma. *J Clin Invest* **94**, 1235–42.

[11] Arteaga CL (1992). Interference of the IGF system as a strategy to inhibit breast cancer growth. *Breast Cancer Res Treat* **22**, 101–106.

[12] Burgaud JL, Resnicoff M, and Baserga R (1995). Mutant IGF-1 receptors as dominant negatives for growth and transformation. *Biochem Biophys Res Commun* **214**, 475–81.

[13] Dunn SE, Ehrlich M, Sharp NJH, Reiss K, Solomon G, Hawkins R, Baserga R, and Barrett JC (1998). A dominant negative mutant of the insulin-like growth factor-1 receptor inhibits the adhesion, invasion, and metastasis of breast cancer. *Cancer Res* **58**, 3353–61.

[14] Andrews DW, Resnicoff M, Flanders AE, Kenyon L, Curtis M, Merli G, Baserga R, Iliakis G, and Aiken RD (2001, April 15). Results of a pilot study involving the use of an antisense oligodeoxynucleotide directed against the insulin-like growth factor receptor in malignant astrocytomas. *J Clin Oncol* **19(8)**, 2189–200.

[15] Delcommenne M, Tan C, Gray V, Rue L, Woodgett JR, and Dedhar S (1998, September). Phosphoinositide-3-OH kinase–dependent regulation of glycogen synthase kinase 3 and protein kinase B/AKT by the integrin linked kinase. *Proc Nat Acad Sci USA* **95**, 11211–16.

[16] Anderson KE, Coadwell J, Stephens LR, and Hawkins PT (1998, June 4). Translocation of PDK-1 to the plasma membrane is important in allowing PDK-1 to activate protein kinase B. *Curr Opin Biol* **8(12)**, 684–91.

[17] Hemmings BA (1997). AKT signaling: linking membrane events to life and death decisions. *Science* **275**, 628–30.

[18] Andjelkovic M, Alessi DR, Meier R, Fernandez A, NJC L, Frech M, Cron P, Cohen P, Lucocq JM, and Hemmings BA (1997, December 12). Role of translocation in the activation and function of protein kinase B. *J Biol Chem* **272**, 51515–24.

[19] Borgatti P, Martelli AM, Bellacosa A, Casto R, Massari L, Capitani S, and Neri LM (2000). Translocation of AKT/PKB to the nucleus of osteoblast-like MC3T3-E1 cells exposed to growth factors. *FEBS Lett* **477**, 27–32.

[20] Dudek H, Datta SR, Franke TF, Binbaum MJ, Yao R, Cooper GM, Segal RA, Kaplan DR, and Greenberg ME (1997). Regulation of neuronal survival by the serine–threonine protein kinase AKT. *Science* **275**, 661–65.

[21] Dunn SE, Torres JV, and Barrett JC (2001, February 15). Up-regulation of urokinase type plasminogen activator by insulin-like growth factor-1 depends upon phosphotidyl inositol-3 kinase and Map kinase kinase. *Cancer Res* **61**, 1367–74.

[22] Dimmmeler S, and Zeiher AM (2000). AKT takes center stage in angiogenesis signaling. *Circ Res* **8**, 4–5.

[23] Zhong H, Chiles K, Feldser D, Laughner E, Hanrahan C, Georgescu MM, Simons JW, and Semenza GL (2000, March 15). Modulation of hypoxia-inducible factor 1 alpha expression by the epidermal growth after phosphatidylinositol 3-kinase/PTEN/AKT/FRAP pathway in human prostate cancer cells: implications for tumor angiogenesis and therapeutics. *Cancer Res* **60**, 1541–45.

[24] Zelzer E, Levy Y, Kahana C, Shilo BZ, Rubinstein M, and Cohen B (1998). Insulin induces transcription of target genes through the hypoxia-inducible factor HIF-1 alpha/ARNT. *EMBO J* **17(17)**, 5085–94.

[25] Cross BAE, Alessi DR, Cohen P, Andjelkovich M, and Hemming BA (1995). Inhibition of glycogen synthase kinase-3 by insulin mediated by protein kinase B Nature. **378**, 785–89.

[26] Du K, and Montminy M (1998, December 4). CREB is a regulatory target for protein kinase AKT/PKB. *J Biol Chem* **273**, 32377–79.

[27] Du K, Asahara H, Jhala US, Wagner BL, and Montminy M (2000, June). Characterization of a CREB gain of function mutant with constitutive transcriptional activity *in vivo*. *Mol Cell Biol* **20(12)**, 4320–27.

[28] Beitner-Johnson D, and Millhorn DE (1998, July 31). Hypoxia induces phosphorylation of the cyclic AMP response element-binding protein by a novel signaling mechanism. *J Biol Chem* **273(31)**, 19834–39.

[29] Pugazhenthi S, Borgas T, O'Conner D, Meintzer MK, Heidenreich KA, and Reusch JE (1999). Insulin-like growth factor-1 mediated activation of the transcription factor cAMP response element-binding protein in PC12 cells. Involvement of p38 mitogen-activated protein kinase–mediated pathway. *J Biol Chem* **274**, 2829–37.

[30] Beitner-Johnson D, Rust RT, Hseih TC, and Millhorn DE (2001). Hypoxia activates AKT and induces phosphorylation of GSK-3 in PC12 cells. *Cell Signalling* **13**, 23–27.

[31] Brunet A, Bonni A, Zigmond MJ, Lin MZ, Juo P, Hu LS, Anderson MJ, Arden KC, Blenis J, and Greenberg ME (1999, March 19). AKT promotes cell survival by phosphorylating and inhibiting a forkhead transcription factor. *Cell* **96**, 857–68.

[32] Kops GJPL, de Ruiter ND, De Vries-Smits AMM, Powell DR, Bos JL, and Burgering BMT (1999). Direct control of the forkhead transcription factor AFX by protein kinase B. *Nature* **398**, 630–34.

[33] Perou CM, Sorlle T, Eisen M, van de Rijn M, Jeffrey SS, Rees CA, Pollack JR, Ross DT, Johnson H, Akslen LA, Fuge O, Pergamenschikov A, Williams C, Zhu SX, Lonning PE, Borresen-Dale A, Brown PO, and Botstein D (2000, August 17). Molecular portraits of human breast tumors. *Nature* **406**, 747–52.

[34] Nuwaysir EF, Mittner M, Trent J, Barrett JC, and Afshari CA (1999). Microarrays and toxicology: the advent of toxicogenomics. *Mol Carcinog* **24**, 153–59.

[35] DeRisi JL, Iyer VR, and Brown PO (1997). Exploring the metabolic and genetic control of gene expression on a genomic scale. *Science* **278**, 680–86.

[36] Chen YC, Dougherty ER, and Bittner ML (1997). Ratio-based decisions and the quantitative analysis of cDNA microarray images. *J Biomed Opt* **2**, 364–74.

[37] Bushel PR, Hamadeh HK, Bennett L, Sieber S, Martin K, Nuwaysir EF, Johnson K, Reynolds K, Paules RS, and Afshsari CA (2001). The Microarray Project System for gene expression experiment information and data validation. *Bioinformatics* **17**, 564–656.

[38] Eisen MB, Spellman PT, Brown PO, and Botstein D (1998). Cluster analysis and display of genome-wide expression patterns. *Proc Nat Acad Sci USA* **95**, 14863–68.

[39] Dunn SE, Torres JV, Nihei N, and Barrett JC (2000). The insulin-like growth factor-1 elevates urokinase-type plasminogen activator-1 in human breast cancer cells: a new avenue for Breast Cancer Therapy. *Mol Carcinog* **27**, 10–17.

[40] Zhang HT, Craft P, Scott PAE, Ziche M, Weich HA, Harris AL, and Bicknell R (1995, Feb 1). Enhancement of tumor growth and vascular density by transfection of vascular endothelial cell growth factor into MCF-1 human breast carcinoma cells. *J Natl Cancer Inst* **87**, 213–19.

[41] Kvietikova I, Wenger RH, Marti HH, and Gassmann M (1995). The transcription factors ATF-1 and CREB-1 bind constitutively to the hypoxia-inducible factor-1 (HIF-1) DNA recognition site. *Nucleic Acids Res* **23(22)**, 4542–50.

[42] Hai T, and Curran T (1991). Cross-family dimerization of transcription factors Fos/Jun and ATF/CREB alters DNA binding specificity. *Proc Natl Acad Sci USA* **88**, 3720–24.

[43] Sterling K, Weaver J, Ho KL, Xu LC, and Bresnick E (1993, September). Rat CYP1A1 negative regulatory element: biological activity and interaction with a protein from liver and hepatoma cells. *Mol Pharmacol* **44(3)**, 560–68.

[44] Marhin WW, Chen S, Facchini LM, Fornace AJJ, and Penn LZ (1997, June 12). Myc represses the growth arrest gene GADD45. *Oncogene* **14(23)**, 2825–34.

[45] Lee TC, Li L, Philipson L, and Ziff EB (1997, November). Myc represses

transcription of the growth arrest gene gas1. *Proc Nat Acad Sci USA* **94(24)**, 12886–91.

[46] Stanhope-Baker P, and Williams BRG (2000, December 8). Identification of connective tissue growth factor as a target of WT1 transcriptional regulation. *J Biol Chem* **275(49)**, 38139–50.

[47] Natch M, Furguson AT, Zhang W, Petroziello JM, Cook BP, Gao YH, Maguire S, Riley D, Cappola G, Landes GM, Madden SL, and Sukumar S (1999, November 1). Combining serial analysis of gene expression and array technologies to identify genes differentially expressed in breast cancer. *Cancer Res* **59**, 5464–70.

[48] Liu D, Rudland PS, Sibson DR, Platt-Higgins A, and Barrachough R (2000, December). Expression of calcium-binding protein S100A2 in breast lesions. *Br J Cancer* **83**, 1473–79.

[49] Bergstraesser LM, Srinivasan G, Jones JC, Stahl S, and Weitzman SA (1995, December). Expression of hemidesmosomes and component proteins is lost by invasive breast cancer cells. *Am J Pathol* **147**, 1823–39.

[50] Byrne C, Coldiz GA, Willett WC, Speizer FE, Pollak M, and Hankinson SE (2000). Plasma insulin-like growth factor-1 (IGF-1), IGF-binding protein 3 and mammographic density. *Cancer Res* **60(60)**, 3744–48.

[51] Guo Y, LJ M, Hanna W, Panerjee D, Miller N, Fishell E, Khokha R, and Boyd NF (2001, March). Growth factors and stromal matrix proteins associated with mammographic density. *Cancer Epidemiol Biomarkers Prev* **10**, 243–48.

[52] Hanahan D, and Folkman J (1996, August 9). Patterns and emerging mechanisms of the angiogenic switch during tumorigenesis. *Cell* **86(3)**, 353–64.

[53] Guidi AJ, Schnitt SJ, Fischer L, Tognazzi K, Harris JR, Dvorak HF, and Brown LF (1997, November 15). Vascular permeability factor (vascular endothelial growth factor) expression and angiogenesis in patients with ductal carcinoma *in situ* of the breast. *Cancer* **80**, 1945–53.

[54] Neufeld G, Cohen T, Gengrinovitch S, and Potorak Z (1999, January). Vascular endothelial growth factor (VEGF) and is receptors. *FASEB J* **13**, 9–22.

[55] DiNardo DN, Butcher DT, Robinson DP, Archer TK, and Rodenhiser DI (2001, August 30). Functional analysis of CpG methylation in the BRCA1 promoter region. *Oncogene* **20(38)**, 5331–40.

[56] Nenoi M, Ichimura S, Mita K, Yukawa O, and Cartwright IL (2001, August 1). Regulation of the catalase gene promoter by Sp1, CCAAT-recognizing factors, and a WR1/Egr-related factor in hydrogen peroxide-resistant HP100 cells. *Cancer Res* **61**, 5885–91.

[57] Ottaviano YL, Issa JP, Parl FF, Smith HS, Baylin SB, and Davidson NE (1994, May 15). Methylation of the estrogen receptor gene CpG island marks loss of estrogen receptor expression in human breast cancer cells. *Cancer Res* **54**, 2552–55.

[58] Schuur ER, McPherson LA, Yang GP, and Weigel RJ (2001, May 4). Genomic structure of the promoters of the human estrogen-alpha gene demonstrate changes in chromatin structure induced by AP2gamma. *J Biol Chem* **276(18)**, 15519–26.

[59] Yang XF, Ferguson ATF, Nass SJ, Phillips DL, Butash KA, Wang SM, Herman JG, and Davidson NE (2000, December 15). Transcriptional activation of estrogen receptor alpha in human breast cancer cells by histone deacetylase inhibition. *Cancer Res* **60**, 6890–94.

[60] Morrow CS, Cowan KH, and Goldsmith ME (1989, January 30). Structure of the human glutathione *S*-transferase p1 gene. *Gene* **75(1)**, 3–11.

[61] Borde-Chiche P, Diedericha M, Morceau F, Puga A, Wellman M, and Dicato M (2001, March 1). Regulation of transcription of the glutathione *S*-transferase P1 gene by methylation of the minimal promoter in human leukemia cells. *Biochem Pharmacol* **61(5)**, 605–12.

[62] Jhaveri MS, and Morrow CS (1998, March 27). Methylation-mediated regulation of the glutathione *S*-transferase P1 gene in human breast cancer cells. *Gene* **210(1)**, 1–7.

[63] Lee KJ, Chan JYC, Lau KF, Lee WC, Miller CCJ, Anderton BH, and Shaw PC (2000). Molecular cloning and expression analysis of human glycogen synthase-3 alpha kinase. *Mol Brain Res* **84**, 150–57.

[64] Kantharidis P, El-Osta A, deSilva M, Wall DM, Hu XF, Slater A, Nadalin G, Parkin JD, and Zalcberg JR (1997, November 3). Altered methylation of the human MDR1 promoter is associated with acquired multidrug resistance. *Clin Cancer Res* **11**, 2025–32.

[65] Ohga T, Uchiumi T, Makino Y, Koike K, Wada M, Kuwano M, and Kohno K (1998, March 13). Direct involvement of the Y-box binding protein YB-1 in genotoxic stress-induced activation of the human multidrug resistance gene-1. *J Biol Chem* **273(11)**, 5997–6000.

[66] Adachi N, Namoto M, Kohno K, and Kyoama H (2000, March 7). Cell-cycle regulation of the DNA topoisomerase II alpha promoter is mediated by proximal CCAAT boxes: possible involvement of acetylation. *Gene* **245(1)**, 49–57.

[67] Kim JC, Yoon JB, Koo HS, and Chung IK (1998, October 2). Cloning and characterization of the 5-flanking regions for the human topoisomerase III gene. *J Biol Chem* **273(40)**, 26130–37.